Properties of gallium-doped hydrogenated amorphous germanium

D. Comedi, F. Fajardo, and I. Chambouleyron
Instituto de Física "Gleb Wataghin", Universidade Estadual de Campinas, Campinas, São Paulo 13083-970, Brazil
(Received 15 February 1995)

The effects of adding small quantities of gallium atoms to hydrogenated amorphous germanium (a-Ge:H) on its dark-conductivity, band-gap, electronic density of states and the hydrogen bonding, were studied in detail by dark-conductivity, optical and infrared-transmission, and photothermal-deflection-spectroscopy measurements. Films of *a*-Ge:H having relative Ga atomic concentrations ranging between 3×10^{-5} and 1×10^{-2} were deposited by the cosputtering of solid Ge and Ga targets in a rf-plasma sputtering chamber. The Ga incorporation was found to produce significant changes in the conductivity in the whole studied concentration range. The sign of the thermopower signal reveals a change from *n*- to *p*-type conduction for Ga concentrations reaching a value of about $(1–5)\times10^{-4}$. No variations in the magnitude of the band gap were detected for Ga atomic concentrations lower than 1×10^{-3}. For higher Ga contents a gradual narrowing of the band gap is observed, which is not correlated by modifications in the hydrogen content nor in the H bonding structure as deduced from the infrared transmission spectra. The present results show that Ga acts as a *p*-type dopant in *a*-Ge:H, with a doping efficiency comparable to that of boron in *a*-Ge:H. The position of the Fermi level with respect to the conduction path levels was determined from the conductivity results, assuming a common constant prefactor for the observed thermally activated dark conductivity for both *n*- and *p*-type samples. The total energy region swept by the Fermi level in the studied Ga concentration range is approximately 0.3 eV, which is about the same as that reported in the literature for B doping of *a*-Ge:H. A semiquantitative electronic density of states distribution for *a*-Ge:H and its evolution with Ga doping was deduced systematically by fitting an analytical model to the optical absorption data. A significant increase in the defect states density was found to develop for Ga contents higher than about 5×10^{-4}. This effect seems to be correlated with the Fermi level approaching the valence-band-tail region. Conductivity prefactors for both electrons and holes in the 140–260 Ω^{-1} cm^{-1}range were deduced from the analysis of the present conductivity and absorption data, which are in fair agreement with values reported in the literature for hydrogenated amorphous silicon and theoretical estimates. Significant tendency for Ga segregation was observed for *a*-Ge:H films having Ga atomic concentrations approaching 1×10^{-2}.

I. INTRODUCTION

Hydrogenated amorphous group-IV semiconductors became the subject of much attention in 1975, when electronic doping of hydrogenated amorphous silicon (*a*-Si:H) was first demonstrated.[1] The role of hydrogen in amorphous semiconductors in passivating a large part of the dangling bonds typically present in these materials, which turned out to be fundamental for the achievement of doping, had been discovered a year before in studies of hydrogenated amorphous germanium (*a*-Ge:H) films prepared by rf-diode sputtering in an argon-hydrogen atmosphere.[2] The following years witnessed a large number of doping studies in *a*-Si:H, which contributed to the development of the first device based on this material, the *a*-Si:H solar cell. The experience accumulated during six years of research of doping in *a*-Si:H was interpreted by Street[3] in 1982. He explained the fact that *a*-Si:H could be substitutionally doped, the observed low doping efficiencies and increasing defect densities with increasing dopant concentration by introducing a model based on a modified version of the 8-N rule previously proposed by Mott.[4] A partial description of the experimental results of doping studies in *a*-Si:H, and a complete treatment of Street's doping model can be found in the book by Street.[5] For the case of *a*-Ge:H, on the other hand, much less work has been done, the main reason being the fact that films of this material exhibit a high density of states in the mobility gap, resulting in low photoconductivity and low photoluminiscence efficiency. Nevertheless, *a*-Ge:H is currently regarded as a natural potential candidate to be used in multijunction solar cells and other hydrogenated amorphous semiconductor-based devices requiring small band-gap components.[6]

Studies of doping in both *a*-Ge:H and *a*-Si:H have been almost exclusively confined to materials doped by adding gases containing the dopant atom to the deposition chamber during deposition of the films by the glow-discharge (gd) method. The *n*-type doping effects of P in gd *a*-Ge:H were observed by Jones *et al.*,[7] using phosphine gas as a dopant source. Later Hauschildt *et al.*[8] studied the dark-conductivity and thermoelectric power in both *n*- and *p*-type gd *a*-Ge:H doped with P and B, using phosphine and diborane gases as dopant sources, respectively. The doping efficiencies for these elements were determined by counting the number of doping-induced excess carriers as inferred from electron spin resonance

(ESR) experiments on doped samples and dividing it by the total concentration of dopant atoms in the films.[9] The doping efficiencies for a-Ge:H were found to be higher than those observed in doped a-Si:H films having the same dopant concentration.[9,10] A different definition of the doping efficiency was then proposed by Stutzmann,[9] which considers the dopant atom concentration in the forming gas in the glow-discharge chamber rather than that resulting in the solid film. From the unified correlation observed between this doping efficiency and the dopant gas concentration in the gd chamber for both a-Si:H and a-Ge:H, Stutzmann deduced that the doping process in these materials is much controlled by details of the plasma-solid interactions, occurring at the growing film surface.[9] This may be expected, on the other hand, from the well-known observation that the optoelectronic properties of intrinsic a-Ge:H and a-Si:H are very sensitive to deposition parameters and specific deposition method employed. In order to derive a general picture of the doping mechanism in tetrahedrally bonded amorphous semiconductors, however, systematic studies of materials doped by using other doping or deposition techniques, or alternative dopant atoms, are highly desirable. These studies should allow one to determine to what extent the effects observed are intrinsic of the doping process itself, or alternatively they depend on the specific doping method or dopant atom employed.

In this work, we report on the changes in the dark-conductivity, optical absorption, and hydrogen bonding of rf-sputtered a-Ge:H, which are induced by adding small quantities of Ga atoms (atomic concentrations lower than $\approx$1%) into the amorphous network. The Ga atoms were introduced by the cosputtering method, using minute amounts of solid Ga placed on top of a crystalline Ge target. The work reported here constitutes a part of a wide program devoted to the systematic study of p-type doping of rf-sputtered a-Ge:H, using atoms from the column III of the Periodic Table as the p-type dopants. Preliminary results of this project have been reported elsewhere.[11] In the present paper, it is shown that Ga acts as a p-type dopant with comparable efficiency as that of B in a-Ge:H, with no changes in the H bonding being apparent. In Sec. III, the changes in the position of the Fermi level induced by the Ga incorporation are determined from the conductivity results by assuming a common constant prefactor for the observed activated conductivity for both electrons and holes. The electronic density of states for the undoped and Ga-doped materials is deduced systematically by fitting an analytical model to the optical absorption data. In Sec. IV, the evolution of the electronic density of states and the Fermi level position within the band gap is discussed. The validity of the method employed for the analysis of the conductivity results is then confirmed by evaluating the conductivity prefactor for both n- and p-type films. The total energy region swept by the Fermi energy in the studied Ga concentration range is deduced to be of 0.3 eV , which is comparable to that observed for B-doped a-Ge:H. Significant Ga-induced narrowing of the optical band gap is observed for Ga atomic concentrations exceeding the 0.1% level.

II. EXPERIMENTAL PROCEDURE

The a-Ge:H films were prepared in a conventional rf-sputtering system in an Ar (99.997%) plus H_2 (99.9995%) atmosphere. A 3-in.-diam., water-cooled, crystalline Ge target (99.9995%) was used. The residual pressure of the chamber was 1×10^{-6} mbar and the substrates were held at 220 °C during deposition. Hydrogen and argon partial pressures of 1.5×10^{-3} and 14.7×10^{-3} mbar, respectively, were used in all deposition runs. The Ga-undoped films exhibited room temperature conductivities of about $(2-3) \times 10^{-5}\ \Omega^{-1}\ \mathrm{cm}^{-1}$ and an optical gap of $E_{04} = 1.2$ eV (i.e, the photon energy for which the absorption coefficient equals $10^4\ \mathrm{cm}^{-1}$). These values are comparable to those reported for a-Ge:H films deposited by glow-discharge[12] and magnetron sputtering.[13] The subgap absorption (50 cm^{-1} for a photon energy of 0.7 eV) and slope of the exponential absorption tail (70 meV), on the other hand, were found to be significantly higher than those reported in the literature for glow-discharge[12,14] and sputtered[13,15] state-of-the-art a-Ge:H (typically $\sim 10-30\ \mathrm{cm}^{-1}$ and $\sim 50-60$ meV, respectively), indicating that the present films had somewhat higher disorder and defect densities.

For the incorporation of Ga into the a-Ge:H films, the Ge target was partially covered by small pieces of solid Ga of varied sizes. The Ga pieces exhibited spherical shape after preliminary deposition runs, indicating that melting of the pieces had occurred, due to the low melting temperature of Ga (29.9 °C). The pieces were therefore placed in small, high purity, Ge receptacles and were presputtered during 30 min before each deposition. This procedure was performed in order to produce a clean and well-defined Ga-sputtered area. The Ga content in the films was varied by varying the relative Ga-to-Ge sputtered areas. The relative Ga-to-Ge atomic concentration ($N_{\mathrm{Ga}}/N_{\mathrm{Ge}}$) for films having Ga concentrations higher than about 1×10^{-3} was directly determined by the proton-induced x ray emission (PIXE) technique, using a 2.4 MeV H^+ beam.[16] The measured $N_{\mathrm{Ga}}/N_{\mathrm{Ge}}$ values were found to scale linearly with the relative Ga-to-Ge relative areas measured by an optical microscope immediatly after each deposition run.[16] The Ga content for films having Ga concentrations below the PIXE detection limit was deduced by extrapolating this linear relationship to the the corresponding lower relative Ga areas.

The substrates used for the deposition of the films were $2 \times 1\ \mathrm{cm}^2$ 7059 Corning glass and polished Si slabs, which were mounted on a grounded substrate holder placed at a distance of 4.5 cm from the targets. The target self bias was -640 V, resulting in a deposition rate of 1.3 Å/s, which did not change significantly for the whole studied sample series. The thickness of the films deposited on the glass substrates was measured by optical interferometry and found to be approximately 1.2 μm.

The dark conductivity was measured on samples deposited onto the glass substrates in a gap-cell configuration, using two coplanar Cr Ohmic contacts separated by 1 mm and an applied voltage of 100 V. The measurements were performed in an oil-free evacuated chamber

in the 150–440 K temperature range, using a Keithley 617 electrometer at a fixed temperature variation rate of 3 K/min. Prior to the measurements, the samples were annealed for a few minutes at 420 K to desorb possible surface contaminants. No differences were observed between the conductivity data taken during heating and cooling of the samples. The sign of the thermopower for these samples was determined by applying a temperature gradient between the Cr contacts and measuring the polarity of the resulting voltage.

Optical transmission measurements in the near infrared and visible region were performed on films deposited on glass substrates. The absorption coefficient was determined from the transmission, using the procedure described by Swanepoel.[17] The subgap absorption was measured in the photon energy range of 0.65 – 1.3 eV, by photothermal-deflection spectroscopy (PDS). The absolute scale of the PDS spectra was determined by matching them to the absorption curves as deduced from the optical transmission measurements. Infrared optical transmission measurements were performed on samples deposited on Si substrates in the 400–4000 cm^{-1} wave-number range, using a Fourier-transform spectrometer. The content of bonded hydrogen in the films was determined from the integrated absorption of the wagging Ge-H mode, following a procedure described in the literature.[18]

Since Ga is known to induce crystallization in *a*-Ge when incorporated at large concentrations,[19] the amorphous character of the samples having the highest Ga content was tested by performing Raman scattering measurements. No signs of crystallization were observed. For the case of the samples having the highest Ga concentration, however, dots of metallic Ga were clearly recognized on the surface of the films by visual inspection. The presence of these dots may indicate a tendency for segregation of the Ga atoms towards the surface or for the formation of Ga clusters at the growing film surface for high Ga contents. While the reason for this behavior is presently not understood, it is interesting to note that it appears to be characteristic of Ga in Ge at these doping levels (i.e., for N_{Ga}/N_{Ge} approaching a value of 1×10^{-2}), as this effect is not observed for *a*-Ge:H films doped with similar atomic concentrations of In and Al, using the same deposition conditions as described above.[11,20] In addition, a tendency for Ga surface segregation in Ga-doped *c*-Ge grown by molecular beam epitaxy has also been reported, which is not observed for the case of B incorporation in similar materials.[21]

III. RESULTS

A. Dark conductivity

Figures 1(a) and 1(b) show the conductivity (σ) as a function of the reciprocal temperature ($1/T$) for a Ga-undoped *a*-Ge:H film and for samples having different Ga contents. It can be seen that for the undoped sample σ exhibits an activated behavior that comprises five orders of magnitude in the 200 – 450 K temperature range [see the solid line in Fig. 1(a)]. As can be seen in Fig. 1(a), adding Ga atoms to the *a*-Ge:H network to a concentration of $N_{Ga}/N_{Ge} = 3.2 \times 10^{-5}$ produces a strong decrease in the conductivity, accompanied by a significant increase in the slope of the σ vs $1/T$ curve. This effect continues up till a concentration of $N_{Ga}/N_{Ge} \approx 1.5 \times 10^{-4}$. For higher Ga contents, the opposite effect is observed; the conductivity increases and the slope becomes less steep [see Fig. 1 (b)]. These results indicate that a Ga-induced shift of the Fermi level (i.e., doping of the material) is occuring. Figure 2 shows the conductivity at room temperature (σ_{RT}) for the whole doped *a*-Ge:H sample series, as a function of the Ga content (N_{Ga}/N_{Ge}). It can be seen that additions of Ga atoms to concentrations of about $N_{Ga}/N_{Ge} \approx 1 \times 10^{-4}$ produce a decrease in σ_{RT} by almost two orders of magnitude down to minimum value of $\sigma_{min} \approx 2.5 \times 10^{-7}\ \Omega^{-1}\,cm^{-1}$. Also shown in the figure is the sign of the thermopower, which for samples in this concentration range is negative, indicating

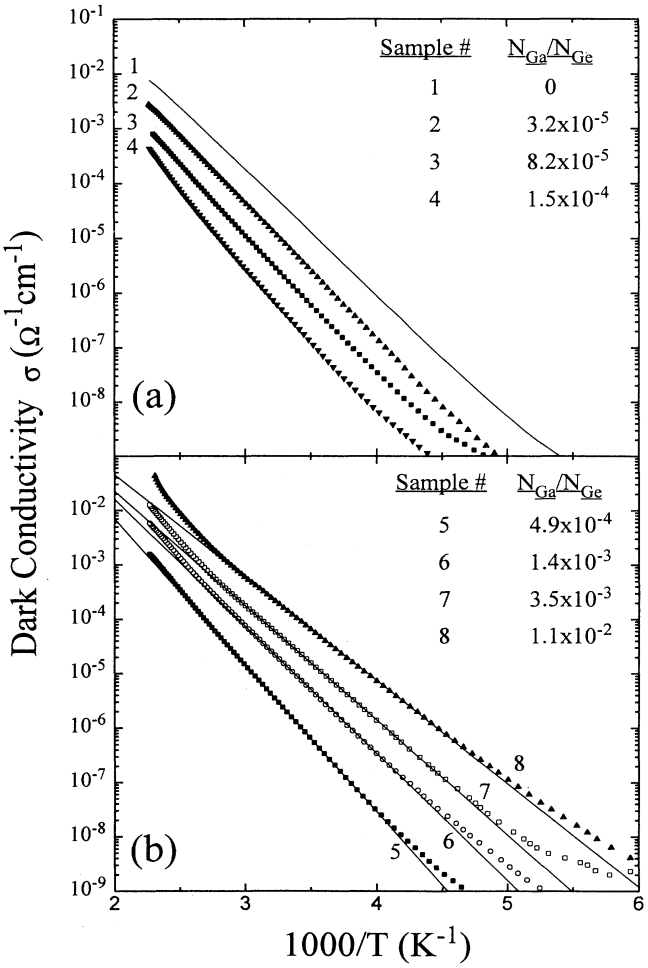

FIG. 1. Dark conductivity σ as a function of the reciprocal temperature $1/T$ for *a*-Ge:H films having different Ga contents. Increasing number label indicates increasing Ga content.

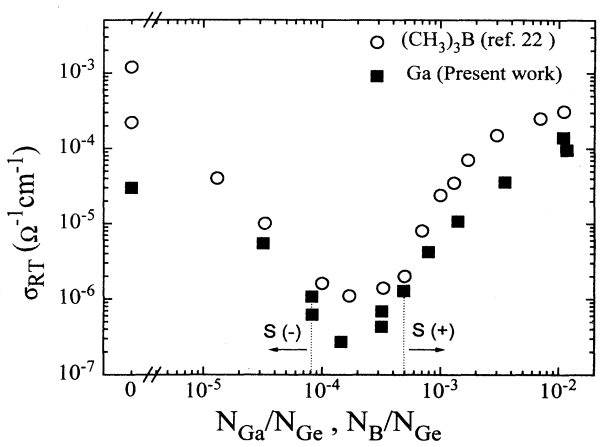

FIG. 2. Conductivity at room temperature (300 K) as a function of the dopant relative atomic concentration in the a-Ge:H film as obtained in the present work for Ga-doped material (squares). The data for B-doped a-Ge:H (circles) corresponds to magnetron sputtered material using $(CH_3)_3B$ gas as a dopant source (taken from Ref. 22). The sign of the thermopower signal S as observed for the present a-Ge:H films is also indicated.

n-type conduction. Hence, the decrease in the conductivity occurring for the lower Ga concentrations can be attributed to a compensation of the initially n-type material by the formation of Ga-induced acceptorlike levels. For samples having Ga contents higher than 1×10^{-4} the conductivity increases, indicating that the Fermi level is shifted below the center of the mobility gap, thus giving rise to increased hole conduction. The sign of the thermopower in this concentration range changes from negative to positive, therefore confirming the setup of p-type conduction. A similar behavior in the room temperature conductivity has been reported for B-doped a-Ge:H deposited by magnetron sputtering and using trimethylborane gas $(CH_3)_3B$ as a dopant source.[22] In Fig. 2, the σ_{RT} data reported in Ref. 22 is compared with the present results for Ga-doped a-Ge:H. As can be seen in the figure, both σ_{RT} data as a function of the dopant concentration follow each other quite well, indicating similar doping efficiency for both dopant atoms. Note, however, that the doping of a-Ge:H using $(CH_3)_3B$ gas results in films containing undesirable significant amounts of[22] C.

As can be seen in Fig. 2, a maximum p-type conductivity at room temperature of about $(1-3)\times10^{-4}$ $\Omega^{-1}\,\mathrm{cm}^{-1}$ is obtained for relative dopant concentrations approaching 1×10^{-2} for both data sets shown. Boron doping of a-Ge:H has been also reported for materials deposited by the glow-discharge technique, using B_2H_6 gas as a dopant source.[8] In these cases, values of σ_{RT} as high as 3×10^{-2} $\Omega^{-1}\,\mathrm{cm}^{-1}$ are achieved for heavy additions of the dopant gas to the deposition chamber. For the case of glow-discharge deposited a-Si:H, the additions of B_2H_6 to the reaction chamber have been found to produce a shrinking of the band gap[23] for B atomic concentrations as low as 5×10^{-4}, which is related to an enhancement of the desorption of H atoms from the films induced by the B.[23,24] Such an effect could be a partial reason for the high conductivities reported for heavily B_2H_6-doped a-Ge:H. Unfortunately, the actual B concentration in the films and the possible variations in the optical gap or in the H concentration accompanying the B-doping process of glow discharge a-Ge:H were not reported in the study of Ref. 8.

As discussed previously, the $\log(\sigma)$ curves for all studied materials show linear behavior when plotted against $1/T$ in conductivity ranges that comprise various orders of magnitude (see Fig. 1). For materials having the highest Ga concentrations, however, a marked concave curvature is observed to develop at high temperatures [see Fig. 1(b)]. A similar effect has been reported for n-type and p-type doped a-Ge:H (Refs. 8, 25, and 26), and a-Si:H.[27] Conductivity measurements performed for samples annealed and cooled at different cooling rates indicate that the observed curvature is related to a transition of the material into a regime, in which significant thermally induced structural equilibration occurs within the time scale of the conductivity measurement.[25,26,28] The temperature above which this effect is observed is associated with the equilibration temperature of the material,[29] which for p-type a-Si:H is about 100 °C, i.e., close to the transition temperatures observed in the conductivity data of Fig. 1(b). At this stage, we confine the analysis of the conductivity to the linear regime in the temperature region that includes the room temperature. This regime is assumed to be characteristic of the material in a state frozen at a temperature close to the equilibration temperature. A study of the conductivity in the equilibration regime would require an independent experimental method, such as the sweep-out experiments described for a-Si:H,[30] for instance, for the determination of the thermally induced changes in the density of electronic shallow states.

From the slopes of the $\log(\sigma)$ vs $1/T$ curves in the linear regime, an activation energy of the conductivity (E_σ) can be deduced. The activation energy of the dark conductivity is given by

$$E_\sigma \approx E_{\mathrm{TR}}^{c}(0) - E_F(0)\ , \tag{1}$$

for n-type samples, with an equivalent expression for p-type materials. Here, $E_{\mathrm{TR}}^{c}(0)$ and $E_F(0)$ represent the conduction path level for the electrons and the Fermi energy values extrapolated from the measured temperature range to $T = 0$ K, respectively. As discussed in the literature,[31] the energy difference between E_F and the conduction path level for electrons (E_{TR}^{c}) or holes (E_{TR}^{v}) at any temperature T in the activated regime can be estimated from the equation

$$|E_{\mathrm{TR}}^{c,v} - E_F| \approx kT \ln\left(\frac{m\sigma_0}{\sigma(T)}\right), \tag{2}$$

where $\sigma_0 \approx 150$ $\Omega^{-1}\,\mathrm{cm}^{-1}$ is the constant exponencial prefactor of the conductivity, assumed to be the same for electrons and holes.[31] The uncertainty in the value of σ_0 is of the order of a factor of 2 as deduced experimentally from dark-conductivity data in a-Si:H (Ref. 28) and theoretically.[31,32] Equation (2) has been slightly modi-

fied by the factor m in the argument of the logarithmic function to account for the possibility of mixed conduction in compensated samples. Thus, $m = 1$ for the case where conduction by a single type of carrier occurs (i.e., for cases where $\sigma_{RT} \gg \sigma_{min}$ at room temperature) and $m \approx 2$ for compensated samples (i.e., samples for which $\sigma_{RT} \approx \sigma_{min}$), for which mixed conduction is assumed to prevail.

In Fig. 3, the $|E_{TR}^{c,v} - E_F|$ values as calculated according to Eq. (2) for $T = 300$ K and $\sigma(T) = \sigma_{RT}$ are plotted together with the corresponding E_σ values as a function of N_{Ga}/N_{Ge}. In the calculations, the value $m = 2$ was used for the films having Ga concentrations corresponding to $N_{Ga}/N_{Ge} \sim 1 \times 10^{-4}$ (data points between the dotted vertical lines in Fig. 3). It can be seen that both $|E_{TR}^{c,v} - E_F|$ and E_σ show an increase for low Ga contents, giving evidence for the Ga-induced shift of E_F from the upper part of the energy gap towards the valence-band edge. For $N_{Ga}/N_{Ge} = (1-3) \times 10^{-4}$, the material is fully compensated and, therefore E_σ and $|E_{TR}^{c,v} - E_F|$ are close to a maximum value, which is about 0.53 eV for $|E_{TR}^{c,v} - E_F|$. For $N_{Ga}/N_{Ge} > 3 \times 10^{-4}$, the material is definitely p type, as shown by the positive sign of the thermopower. In this concentration range, E_σ and $|E_{TR}^{c,v} - E_F|$ are both reduced, indicating a further shift of E_F towards the valence-band edge.

Assuming that the maximum observed value of $|E_{TR}^{c,v} - E_F|$ of about 0.53 eV corresponds to the case in which the Fermi level is close to the center of the mobility gap E_g^μ, and that the transport path levels E_{TR}^c and E_{TR}^v coincide with the respective conduction- and valence-band mobility edges, a value for E_g^μ of 1.06 eV is deduced. This result is between those estimated by the same method for magnetron sputtered[22] ($E_g^\mu \simeq 1.0$ eV) and glow-discharge[33] a-Ge:H ($E_g^\mu \simeq 1.1$ eV) a-Ge:H. In addition, the E_g^μ value is in overall agreement with the optical gap of the material as measured by optical transmission, as will be shown in the next section. This result suggests that the interpretation of the dark-conductivity data in terms of Eq. (2) with a conductivity prefactor $\sigma_0 \approx 150\ \Omega^{-1}\,\mathrm{cm}^{-1}$ for both electrons and holes is consistent with the present data. This point will be discussed in some more detail in Sec. IV.

B. Optostructural properties

In contrast to the conductivity results, the optical properties of Ga-doped a-Ge:H show little changes upon small and moderate additions of Ga into the amorphous network. Figure 4 shows the absorption coefficient as determined by optical transmission and PDS measurements, as a function of the photon energy for samples having different Ga contents. The interference fringes typically appearing in the absorption spectra were averaged out for clarity. As can be appreciated from the figure, for N_{Ga}/N_{Ge} values of up to 1.5×10^{-4}, no significant Ga-induced changes in the entire absorption curves are observed. For higher Ga contents, an increase in the absorption in the subgap and tail regions is clearly detected. For N_{Ga}/N_{Ge} values higher than about 2×10^{-3}, significant Ga-induced modifications in the region of high absorption start to appear as well, which show up as a gradual shift of the absorption curve to lower energies [see data for sample 4 ($N_{Ga}/N_{Ge} = 1.1 \times 10^{-2}$) in Fig. 4]. Note that for samples having Ga contents approaching this high concentration regime ($\sim 1 \times 10^{-2}$) the corresponding data should be taken with some care, as a significant tendency for Ga segregation was observed in these films. It should be pointed out, however, that simi-

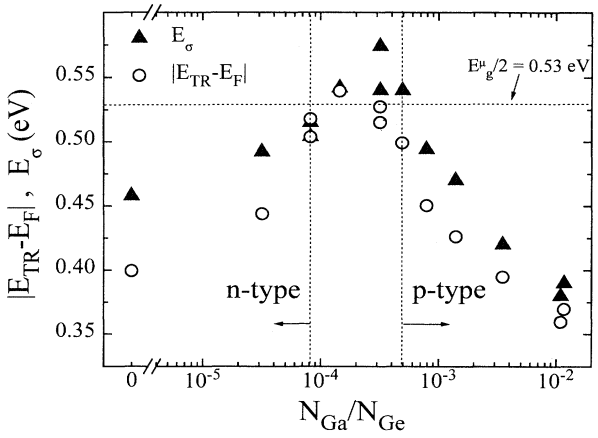

FIG. 3. Activation energy of the dark conductivity (E_σ) as determined from the slope of the linear regions in Fig. 1 (triangles) and the Fermi level position, with respect to the conduction path levels $|E_{TR}^{c,v} - E_F|$ as calculated from the room temperature conductivity data, using Eq. (2) (circles), as a function of the relative Ga concentration, N_{Ga}/N_{Ge}.

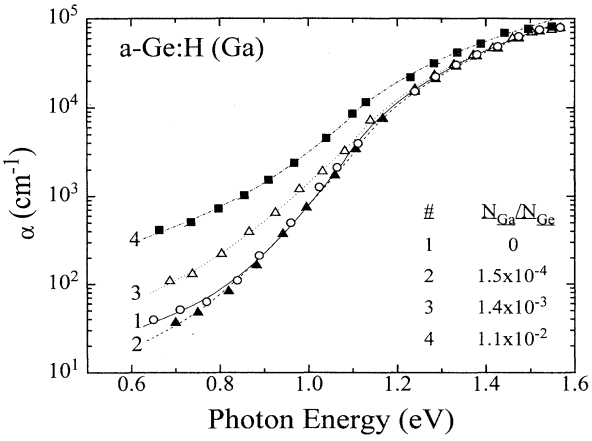

FIG. 4. Optical absorption coefficient as determined by optical transmission and PDS (symbols), as a function of the photon energy for a-Ge:H films having different Ga contents. The lines are theoretical fits to the data points using a model described in the text.

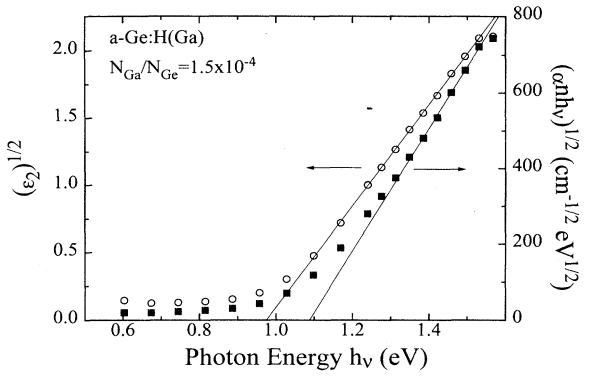

FIG. 5. Square root of the imaginary part of the dielectric coefficient (circles) and $(\alpha n h\nu)^{1/2}$ (squares) as determined by optical transmission for an a-Ge:H film having a Ga relative concentration of $N_{Ga}/N_{Ge} = 1.5 \times 10^{-4}$, as a function of the photon energy $h\nu$. The lines are straight-line fits to the corresponding data points in the 1.35–1.52 eV photon energy region.

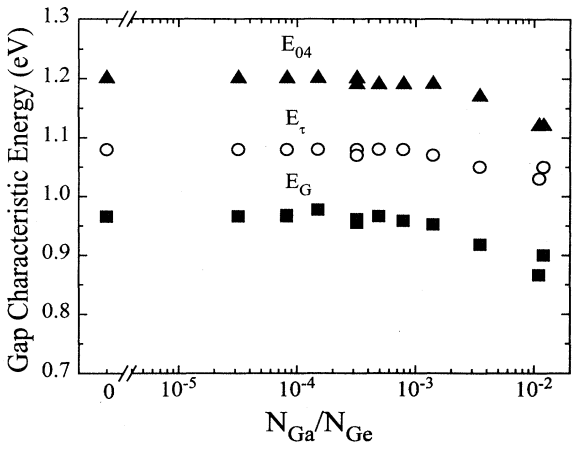

FIG. 6. Band-gap characteristic energies E_{04}, E_τ, and E_G as determined from the absorption data for the studied a-Ge:H films, as a function of the Ga concentration. Note that all three parameters show a gradual narrowing of the band gap for $N_{Ga}/N_{Ge} > 1.4 \times 10^{-3}$.

lar band-gap narrowing effects have been observed by our research group in a-Ge:H films doped with comparably high In and Al contents, with no indications for metallic segregation being apparent in these cases.[20]

In order to systematically quantify the effects observed in the absorption curves shown in Fig. 4, we analyze the data in terms of the Tauc model in the dipole-matrix-element representation.[34] Cody *et al.*[35] showed that in this representation the energy-independent matrix-element approximation leads to better agreement with the experimental data than in the momentum representation used originally by Tauc.[36] In this model, the absorption is represented by the imaginary part of the dielectric function ϵ_2, which is related to the absorption coefficient α through the film refractive index n and the photon energy $h\nu$ according to $\epsilon_2 = \hbar c \alpha n/(h\nu)$. For the band-band optical transitions in this representation, assuming parabolic occupied (valence band) and unoccupied (conduction band) electronic density of states,

$$N_{c,v}(E) = N^0_{c,v}(E - E_{c,v})^{1/2} , \tag{3}$$

where $N^0_{c,v}$ and $E_{c,v}$ are constants, the following parabolic expression for the imaginary part of the dielectric function is obtained:[34]

$$\epsilon_2^{BB} = K_{BB}(h\nu - E_G)^2, \tag{4}$$

where K_{BB} is a constant and $E_G = E_c - E_v$ is a gap energy, which can be determined experimentally by extrapolating Eq. (4) to $\epsilon_2^{BB} = 0$. In Fig. 5, $(\epsilon_2)^{1/2}$ has been plotted as a function of $h\nu$ for one of the doped a-Ge:H samples. The Tauc $(\alpha n h\nu)^{1/2}$ vs $h\nu$ form has also been included in the figure for comparison. It can

TABLE I. Parameters obtained from the fitting of the model described in the text to the absorption coefficient data for a-Ge:H films having different Ga concentrations.

N_{Ga}/N_{Ge}	E_G (eV)	K_{BB} (eV^{-2})	E_0^V (meV)	$\rho_D/N^0_{c,v}$ ($\times 10^{-4}$ eV$^{3/2}$)
0	0.97	13.9	71	2.3
3.2×10^{-5}	0.97	13.6	71	1.8
8.2×10^{-5}	0.97	13.8	72	1.6
8.2×10^{-5}	0.97	14.0	69	3.4
1.5×10^{-4}	0.98	14.3	78	1.3
3.2×10^{-4}	0.96	13.9	78	2.0
3.2×10^{-4}	0.96	13.2	75	2.8
4.9×10^{-4}	0.97	13.9	78	2.5
7.9×10^{-4}	0.96	13.8	78	6.0
1.4×10^{-3}	0.95	13.6	95	43
3.5×10^{-3}	0.92	11.9	100	100
1.2×10^{-2}	0.90	15.1	100	200
1.1×10^{-2}	0.87	14.8	100	450

be seen that, as has been previously noted for a-Si:H,[35] the present data plotted in the $(\epsilon_2)^{1/2}$ form are found to be in very good agreement with a linear fit over a wider energy range than for the case of the $(\alpha nh\nu)^{1/2}$ plot. The results for the parameters E_G and K_{BB} for the samples studied in the present work obtained by fitting the absorption coefficient data using Eq. (4) are compiled in Table I. Figure 6 shows the gap characteristic energies E_G, E_{04} (the photon energy for which $\alpha = 10^4$ cm^{-1}), and E_τ [as determined by extrapolation to $\alpha = 0$ of the $(\alpha nh\nu)^{1/2}$ vs $h\nu$ curve, see Fig. 5] as a function of the Ga content, $N_{\rm Ga}/N_{\rm Ge}$. It can be seen that up to $N_{\rm Ga}/N_{\rm Ge}$ values of approximately 1.5×10^{-3}, the gap characteristic energies remain essentially unmodified. This is in contrast to the conductivity results discussed in the previous subsection, which show significant changes in the whole studied Ga concentration range. Hence, it can be concluded that the changes in conductivity are mainly due to Ga-induced shifts of the Fermi level within the band gap and not due to changes in the band gap itself, in agreement with the interpretation adopted in the previous section. Note, in addition, that the mobility gap as determined from the room temperature conductivity and Eq. (2) ($E_g^\mu = 1.06$ eV) is in good overall agreement with the Tauc optical gap energy shown in Fig. 6. As can also be seen in the figure, for $N_{\rm Ga}/N_{\rm Ge} > 1.5 \times 10^{-3}$, a gradual narrowing of the optical gap with increasing Ga content is observed for all three gap characteristic energies shown. This behavior will be discussed in the next section.

The Ga-induced changes in the subgap absorption of the Ga-doped a-Ge:H films is next considered. As it can be noted in the absorption curves shown in Fig. 4, significant modifications in the subgap absorption exist for moderate and high Ga incorporation. From the curves, it is possible to extract the slope of the exponential absorption tail (the Urbach tail E_0), which is usually assumed to be determined by optical transitions between an exponential valence-band tail of equal slope and the conduction band. The absorption coefficient for a photon energy of 0.7 eV ($\alpha_{0.7}$), on the other hand, has been proposed as a useful parameter to determine the dangling bond density through a calibration constant based on PDS and ESR measurements performed in undoped samples.[37] It should be noted, however, that large uncertainties are involved in the direct determination of E_0, due to the reduced exponential region observed typically in a-Ge:H (see Fig. 4). In addition, significant artificial coupling between E_0 and $\alpha_{0.7}$ could result from contributions from the subgap absorption to the exponential tail region and vice versa. In order to minimize this uncertainty and to systematically derive the Ga induced modifications in the band-tail slope and defect density, a method described in detail by Cody[34] is adopted to fit the full absorption curves such as shown in Fig. 4. A model density of states composed of parabolic valence and conduction bands [see Eq. (3)] including exponential tails and a single, discrete, defect level is assumed. The total imaginary dielectric function is given by

$$\epsilon_2 = \epsilon_2^{\rm BB} + \epsilon_2^{\rm TB} + \epsilon_2^{\rm SB} , \qquad (5)$$

where the superscripts BB, TB, and SB stand for band-to-band, tail-to-band, and defect states-to-band optical transitions, respectively. The defect states are assumed to be due to Ge dangling bonds observed by ESR measurements,[38] which can be empty, singly, or doubly occupied. Adjustable parameters in this model are the characteristic energy E_0^V of the exponential valence-band tail (the corresponding conduction-band-tail slope E_0^C is neglected at this stage), the volume density of deep states (ρ_D) relative to the parabolic band parameter N_c^0 or N_v^0, as defined by Eq. (3) (i.e., ρ_D/N_v^0 for n-type and ρ_D/N_c^0 for p type, respectively[34]), and the energy position of

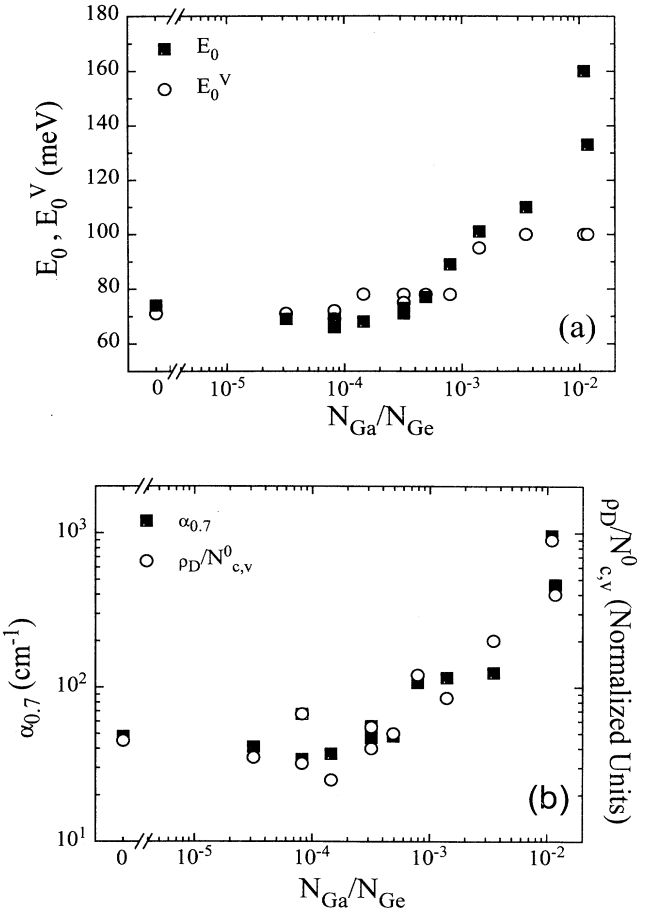

FIG. 7. (a) Urbach energy E_0 (squares) as measured directly from the slope of the exponential absorption tail, and the band-tail slope parameter E_0^V as determined by the fitting of the model described in the text (circles) to the entire absorption curves, as a function of the Ga relative atomic concentration in the a-Ge:H film, $N_{\rm Ga}/N_{\rm Ge}$. (b) Absorption coefficient for a photon energy of 0.7 eV ($\alpha_{0.7}$, squares), and the $\rho_D/N_{c,v}^0$ parameter as determined by the fitting of the model described in the text (circles) to the entire absorption coefficient curves, as a function of $N_{\rm Ga}/N_{\rm Ge}$. The values of $\rho_D/N_{c,v}^0$ (taken from Table I) were multiplied by a constant factor in order to facilitate their comparison with the corresponding $\alpha_{0.7}$ data.

these states with respect to the band edge to which (or from which) the optical transition occurs (E_D). In principle, various defect levels having different values for E_D may occur. For the n-type samples, for instance, we expect the defect states to be doubly occupied, and hence transitions from the valence band to these states will be inhibited. In this case, we expect transitions from the doubly occupied defect state into the conduction band (with a corresponding transition energy E_D value denoted by E_D^-) to play a dominant role in the determination of the subgap absorption. Similarly, for p-type samples, many of the defect states will be empty, and, therefore, only transitions from the valence band into these states (with a corresponding E_D value denoted by E_D^+) will need to be considered. The model is found to fit the present absorption data very well, as can be appreciated by the excellent agreement between the lines and the data points in Fig. 4. These fits were obtained by keeping $E_D^- = E_D^+ = E_D$ fixed at a value of 0.4 eV (i.e., close to midgap position), while taking E_0^V and $\rho_D/N_{c,v}^0$ as adjustable parameters. The effects of changing E_D was tested using $E_D = 0.5$ eV, this value was found to produce somewhat worse fits with few percent induced variations in the results obtained for E_0^V and $\rho_D/N_{c,v}^0$. The results of the fitting procedure for the whole series of the doped a-Ge:H samples are also compiled in Table I. Figures 7(a) and 7(b) show E_0^V and $\rho_D/N_{c,v}^0$ plotted against $N_{\rm Ga}/N_{\rm Ge}$. Also shown in the figures are the corresponding values of the Urbach energy E_0 (as determined by the slope of the absorption curve) and $\alpha_{0.7}$. Both figures show negligible or no variations in the plotted quantities up to $N_{\rm Ga}/N_{\rm Ge} \approx 4 \times 10^{-4}$. For higher Ga contents the band-tail slope, the Urbach energy, $\alpha_{0.7}$ and $\rho_D/N_{c,v}^0$ increase, indicating increasing disorder induced by the addition of the Ga into the a-Ge:H network, with a corresponding increase in the number of defects, which give rise to the subgap absorption. Note that the data points for $\alpha_{0.7}$ are found to be in good agreement with $\rho_D/N_{c,v}^0$ in the whole Ga concentration range, indicating a very small contribution of the absorption tail at a photon energy of 0.7 eV, thus justifying the use of $\alpha_{0.7}$ as a measure of defect absorption.[37] The band-tail parameter E_0^V, on the other hand, is found to be smaller than the Urbach energy for films having Ga concentrations $N_{\rm Ga}/N_{\rm Ge} > 1\times10^{-3}$, giving evidence for significant contributions from the defect absorption to the slope of the absorption curves in the tail region.

IV. DISCUSSION

A. Density of state distribution and Fermi energy

With the results just presented, we are in a situation in which the evolution of the electronic density of states (DOS) and the Fermi level position with increasing Ga content in a-Ge:H can be deduced in a semiquantitative way. For materials having Ga concentrations in the $0 \le N_{\rm Ga}/N_{\rm Ge} < 4 \times 10^{-4}$ range, the absorption data shows small changes, indicating small or no Ga-induced changes in the DOS. The estimated one-electron DOS for these samples is plotted in Fig. 8(a) (curve I). The reference of energy is the valence-band edge, which in the model used for the analysis of the absorption data is the point at which $N_v(E_v \equiv 0) = 0$ [see Eq. (3)]. The defect level, which represents the singly occupied Ge dangling bonds as observed by ESR,[38] is placed at about $E_d^0 = 0.5$ eV. This position is in agreement with that deduced from the ESR measurements and is consistent with the value of $E_D^- = E_c - E_d^- = E_G - (E_d^0 + U) \approx 0.4$ eV found to produce a good fit of the defect-band absorption data for n-type samples (see Sec. III B). Here, $U = 0.1$ eV is the correlation energy for the defect states, which has been determined for a-Ge:H by the ESR experiments.[38] The defect peak has been gaussian broadened with a standard deviation of 0.08 eV, in consistency with the ESR results. The area below the defect peak is chosen to reproduce a total volume defect density ρ_D of 4.5×10^{17} cm^{-3}, which can be deduced from the measured subgap absorption coefficient $\alpha_{0.7}$ [taken from Fig. 7(b)] and a calibration constant reported in the literature.[37] From this value of ρ_D and the ratio $\rho_D/N_v^0 \approx 2.3 \times 10^{-4}$ eV$^{3/2}$ as determined from the analysis of the absorption data (see Table I), a value for N_v^0 of 2×10^{21} cm^{-3} eV$^{-3/2}$ can be deduced, from which the valence-band shoulder of the DOS distribution is estimated [using Eq. (3)]. This value of N_v^0 is in excellent agreement with that used by others to fit the absorption curves for a-Si:H.[39] The valence-band tail is calculated using the deduced value for E_0^V from Table I. Finally, the conduction band is constructed schematically, taking into account the determined value for E_G (from Table I), assuming $N_c^0 = N_v^0$. A conduction-band-tail slope of $E_0^C = 0.6E_0^V$ is assumed, which is consistent with ESR results[38] for n-type doped a-Ge:H films, and also with the fact that the conductivity activation energies observed for heavily n-type doped a-Ge:H (Ref. 40) are significatly smaller than those achievable by heavy p-type doping. The position of the transport path levels $E_{\rm TR}^{c,v}$ [shown as solid vertical lines in Fig. 8(a)] is estimated using the mobility gap value of $E_g^\mu = 1.06$ eV, as deduced from the minimum conductivity value (see Sec. III A). Here, we assume an equal DOS value at both $E_{\rm TR}^c$ and $E_{\rm TR}^v$, which turns out to be about 3×10^{20} cm^{-3} eV^{-1}. This value is in good agreement with those reported for DOS distributions also deduced from combined absorption and conductivity data for glow-discharge a-Ge:H (Ref. 41) and a-Si:H (Ref. 42). Note, however, that for the case of a-Si:H, electron photoemission combined with time-of-flight experiments yield a corresponding value, which is about an order of magnitude larger.[5] The reason for this discrepancy could be the assumption of energy-independent transition matrix elements used for the analysis of the absorption curves.

Also shown in Fig. 8(a) are the resulting Fermi level positions as deduced from the conductivity data (see also Fig. 3). As can be seen in the figure, the Fermi level is swept by the Ga doping from its initial value $E_F(0)$ for the Ga-undoped a-Ge:H film towards the valence band. For the sample having a Ga concentration of $N_{\rm Ga}/N_{\rm Ge} = 5 \times 10^{-4}$, the Fermi level reaches the position denoted by $E_F(1)$ in Fig. 8(a), which is just below midgap and p-type conduction starts to set in. For

$N_{Ga}/N_{Ge} > 5 \times 10^{-4}$ (i.e., as E_F definitely enters into the lower part of the gap), significant modifications in the DOS distribution are inferred from the absorption data. Curve II in Fig. 8(a) shows the DOS distribution as estimated for a-Ge:H with $N_{Ga}/N_{Ge} = 1.4 \times 10^{-3}$, assuming that the changes in the subgap absorption parameter ($\rho_D/N^0_{c,v}$, see Table 1) are due to changes in the defect density ρ_D only. The corresponding Fermi level position is shown by $E_F(2)$, which at this stage reaches the valence-band-tail region. The DOS distributions deduced for materials with $N_{Ga}/N_{Ge} > 1.4 \times 10^{-3}$ are shown in Fig. 8(b). It can be seen that, together with a gradual increase in the DOS in the subgap region, significant modifications in the tail and shoulder regions are deduced, which are related to the slight reduction of the optical gap observed for these heavily doped samples (see Fig. 6 and Table I). For the a-Ge:H film with $N_{Ga}/N_{Ge} = 1.1 \times 10^{-2}$ [curve IV in Fig. 8(b)], which is about the highest Ga concentration studied in the present work, the Fermi level reaches a distance from the valence-band edge of 0.36 eV [$E_F(4)$ in Fig. 8(b)]. Hence, the total energy region swept by the Fermi level in the whole studied Ga concentration range of $0 \leq N_{Ga}/N_{Ge} < 1.2 \times 10^{-2}$ is about 0.3 eV. This is close to the value observed for glow-discharge deposited a-Ge:H doped by B_2H_6, for which E_σ is observed to change from 0.5 eV down to a minimum value of about[8,10] 0.15 – 0.2 eV. Note, however, that both results are significantly larger than the corresponding total Fermi energy shift of about 0.2 eV, as measured by photoelectron spectroscopy for B_2H_6 doped a-Ge:H.[43]

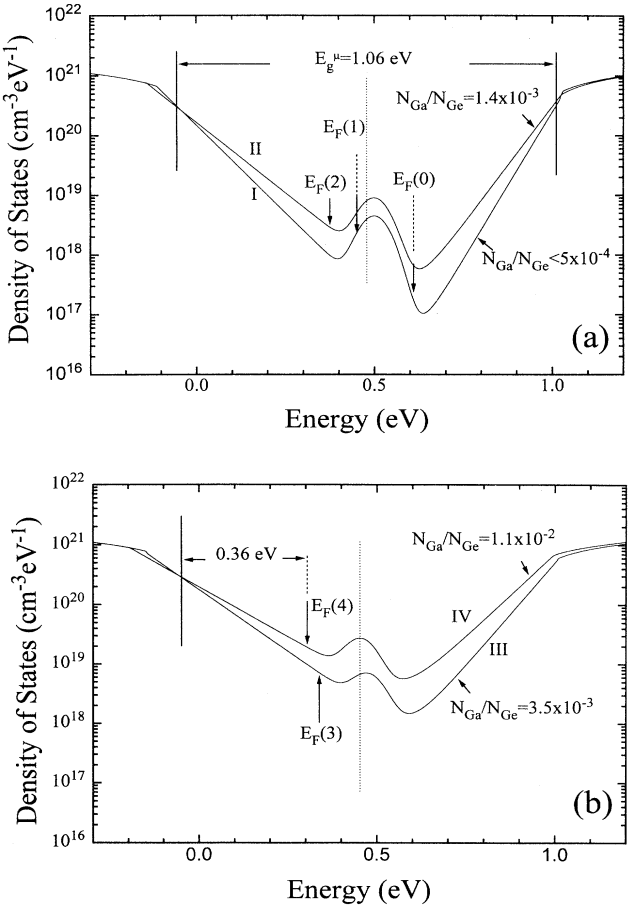

FIG. 8. Semiquantitative electronic density of states distribution as deduced from the fitting of the model described in the text to the absorption coefficient curves for a-Ge:H films having different Ga concentrations. The vertical solid and dotted lines indicate the estimated positions for the conduction path levels and the center of the mobility gap, respectively. The arrows show the estimated position of the Fermi level for the different doping levels: $E_F(0)$ is for the undoped sample, $E_F(1)$ for $N_{Ga}/N_{Ge} \sim 5 \times 10^{-4}$, $E_F(2)$ for $N_{Ga}/N_{Ge} = 1.4 \times 10^{-3}$, $E_F(3)$ for $N_{Ga}/N_{Ge} = 3.5 \times 10^{-3}$, and $E_F(4)$ for $N_{Ga}/N_{Ge} = 1.1 \times 10^{-2}$.

It is interesting to note the fact that the significant structural modifications as deduced from the absorption data start to appear when the Fermi energy enters the lower part of the band gap. A similar effect has been observed for B-doped glow-discharge a-Ge:H (Ref. 33) and a-Si:H.[42] This effect clearly shows a correlation between the Fermi level position and the density of structural defects in the p-type side, such as that expected from weak bond-dangling bond-conversion models proposed for a-Si:H.[44] Note, however, that the density of doping-induced defects increases almost linearly with increasing dopant concentration in the films for $N_{Ga}/N_{Ge} > 5 \times 10^{-4}$ [see Fig. 7(b)]. This is different than the square-root dependence of the defect density on the concentration of dopant species in the forming gas typically observed in P- and B-doped a-Si:H deposited by the glow-discharge method.[3,10] For the case of a-Ge:H, on the other hand, this dependence is not well established. The correlation between the defect density and the Fermi level position as observed for the present materials, as well as its dependence on the dopant concentration, will be treated in a forthcoming publication.

B. Hydrogenation

The infrared spectra measured for the whole studied sample series show features corresponding to the wagging and stretching Ge-H vibrational modes as previously reported for a-Ge:H.[45] The integrated intensity of the wagging mode, which appears at a wave number of 564 cm^{-1}, was found to remain unchanged with Ga incorporation in the whole studied Ga concentration range. Using the calibration constant reported in the literature,[18] an atomic concentration of bonded hydrogen of about 5.5% is found, which is about the same as that observed in the magnetron sputtered a-Ge:H films used for B doping by trymethilboron gas.[22] The peak corresponding to the stretching mode shows the splitting into two components centered at about 1870 and 1970 cm^{-1} wave numbers, respectively, as previously reported for a-Ge:H.[45] The component at lower wave number (the "bulk" mode) has been attributed to insterstitial H atoms bonded to Ge atoms in the bulk. The component at the higher wave

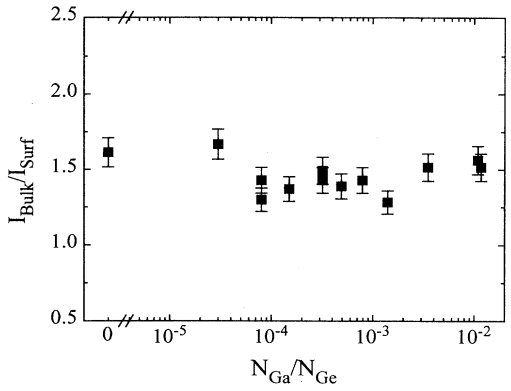

FIG. 9. Ratio of the integrated intensities of the peaks corresponding to the "bulk" and "surface" Ge-H vibrational stretching modes (observed in the infrared absorption spectra at wave numbers of 1870 and 1970 cm^{-1}, respectively), as a function of the Ga relative atomic concentration, N_{Ga}/N_{Ge}.

number (called the "surface" mode), on the other hand, has been interpreted as being due to H atoms bonded to internal surfaces, which constitute the boundaries of voids typically existing in these materials.[45] The changes in the ratio of the integrated intensities of the surface and bulk modes are, therefore, believed to represent the changes in the effective void density in the films. Figure 9 shows the bulk mode-surface mode ratio as a function of the Ga content, N_{Ga}/N_{Ge}. It can be seen that, within the experimental scattering in the data, the ratio remains unmodified in the whole Ga concentration region. From this result and the constant observed intensity of the wagging mode, it can be concluded that no significant modifications in the H bonding structure nor in the void density are induced by the Ga incorporation into the a-Ge:H network.

C. Estimation of the conductivity prefactor

The values for the Fermi level position as determined from the conductivity results depend to some extent on the validity of Eq. (2) and the assumption of a constant prefactor for the conductivity for both electrons and holes of $\sigma_0 \approx 150\ \Omega^{-1}\,cm^{-1}$ used in Sec. III A. This assumption, in addition, has been used in the present work and by others[22,33] to deduce a value for the mobility gap of the material. In this subsection, the above assumption is tested for the present data by comparing the conductivity prefactors σ_0^*, which are determined experimentally by extrapolating the linear σ vs $1/T$ plots to $1/T = 0$, with the quoted value for σ_0. For the case of doped and undoped a-Si:H, it has been shown that the observed differences between σ_0^* and σ_0 arise mainly due to the temperature dependence of the Fermi energy and other energy levels within the mobility gap.[28,31] To a first order approximation, the relation between σ_0 and σ_0^* in such a case should be given by[5]

TABLE II. Calculated rate of variation with temperature of E_F (γ_F) and $|\,E_{TR}^{c,v} - E_F\,|$ (γ_F) (both in units of k, the Botzmann constant) and the corresponding conductivity prefactor σ_0 as calculated from the experimental σ_0^* values using Eq. (6), for a-Ge:H films having different Ga concentrations.

N_{Ga}/N_{Ge}	$\sigma_0^*(\Omega^{-1}\,cm^{-1})$	$\gamma_F(k)$	$\gamma_G(k)$	$\sigma_0(\Omega^{-1}\,cm^{-1})$
0	1550	-0.43	-1.50	225
1.4×10^{-3}	862	0.41	-1.61	258
3.5×10^{-3}	362	0.81	-1.49	183
1.1×10^{-2}	305	0.58	-1.36	140

$$\sigma_0 \approx \sigma_0^* \exp\left[-(\gamma_F + \gamma_G)/k\right], \tag{6}$$

where k is the Boltzmann constant. Here, γ_F represents the rate of variation of the Fermi energy with temperature due to the statistical shift, and γ_G is the rate of change in $|E_{TR}^{c,v} - E_F|$, due to the temperature dependence of the band gap. Table II shows the σ_0 values estimated from the measured conductivity prefactors σ_0^* for some of the studied a-Ge:H samples, using Eq. (6). The values of γ_G were calculated assuming the scaling relation[5] $\gamma_G = \frac{|E_{TR}^{c,v} - E_F|}{E_g^o}\gamma_{op}$, where $\gamma_{op} \approx 4k$ is the temperature dependence coefficient reported for the optical gap of a-Ge:H.[31] The values of γ_F were estimated by calculating the statistical shift, using the DOS distributions shown in Figs. 8(a) and 8(b) and full Fermi statistics, taking into account the correlation energy of 0.1 eV for doubly occupancy of the defect levels, but neglecting the significantly smaller correlation energy for the band-tail states.[38] As can be seen in Table II, the estimated values of σ_0 are in the 140–260 $\Omega^{-1}\,cm^{-1}$ range, which are in fair agreement with the previously assumed value $\sigma_0 \approx 150$ $\Omega^{-1}\,cm^{-1}$. Note that similar values of σ_0 are obtained for the samples considered, regardless whether they are n-type (for the Ga-undoped a-Ge:H film) or p type (for the Ga-doped samples shown in Table II). This fact supports the idea of approximately equal σ_0 for electrons and holes and the procedure of using this assumption for the estimation of the Fermi level position and the mobility gap. While the present result agrees with theoretical arguments[31] and similar experimental data for a-Si:H,[28] it is at odds with the conclusions of the work by Hauschildt *et al.* in B- and P-doped a-Ge:H, who interpreted their experimental transport data in a-Ge:H, by invoking a σ_0 for holes larger by an order of magnitude than for electrons.[8]

D. Concluding remarks

It has been shown that upon additions of Ga into a-Ge:H significant changes in the conductivity are measured. The optical band gap for $0 \le N_{Ga}/N_{Ge} < 1.4 \times 10^{-3}$ is not modified by Ga, indicating that the observed changes in the conductivity are due to shifts in the Fermi energy produced by Ga acceptorlike states in the valence-band-tail region. For higher Ga contents, a

small reduction of the band gap is detected, which contributes slightly to the conductivity increase observed in this concentration region. The infrared data shows that this effect is not related to a reduced hydrogenation of the material induced by Ga, in contrast to what was reported for B_2H_6 doped glow-discharge a-Si:H.[23] In the present case, the band-gap reduction appears to be associated with the increasing bonding and structural disorder introduced by the Ga. This disorder is primarily reflected by the increase in the band-tail slope parameter E_0^V for moderate and high N_{Ga}/N_{Ge} values, as shown in Fig. 7(a). The increasing defect density usually observed with increasing doping level in hydrogenated amorphous semiconductors[33,42] [see also Fig. 7(b)] can be understood in the framework of weak bond-dangling bond-conversion models, such as those proposed by Street and Winer[44] and Stutzmann,[46] for a material having a given valence-band tail, which is assumed to represent a weak-bond reservoir for dangling bond creation. However, the mechanism leading to the increase in the valence-band-tail slope itself, as usually observed with increasing doping level in a-Si:H and a-Ge:H [and also in Fig. 7(a)], is not considered in these models. One source of structural disorder leading to the increase in the slope of band tails is probably the increasing number of dangling bonds induced by doping[3,46] and the associated expected relaxation of lattice sites in the vicinity of these bonds. However, an important source of bonding and structural disorder, which should be considered, is the large number of nonactive impurities incorporated, which for the case of Ga are expected to be bonded in sp^2 configurations, in contrast to the Ge–Ge sp^3 hybrids characteristic of the a-Ge:H network. Since the doping efficiencies in amorphous semiconductors are typically of the order of[5,9,10] 1%, the great majority of the incorporated Ga atoms will contribute to this disorder by increasing the overall width of the network bond length and bond angle distributions and hence the slope of the band tails. For sufficiently high amounts of Ga atoms in the amorphous network, modifications at both band edges may also occur, thus producing the observed overall band-gap narrowing. Clearly, more work should be done in trying to identify the mechanism of Ga-induced band-gap narrowing observed for high Ga incorporation, which appears to be general to other p-type dopants in a-Ge:H.[20]

V. SUMMARY

In this work, the changes in the dark conductivity, optical absorption, and hydrogen bonding of rf-sputtered a-Ge:H, which are induced by adding small quantities of Ga atoms ($3.2\times10^{-5} < N_{Ga}/N_{Ge} < 1.2 \times 10^{-2}$) into the amorphous network, were studied in detail. The following changes were found.

(1) Ga acts as a substitutional dopant in rf-sputtered a-Ge:H, with a doping efficiency comparable to that of B in a-Ge:H.

(2) No changes in the magnitude of the band gap are observed for $0 \leq N_{Ga}/N_{Ge} < 1.4 \times 10^{-3}$. For higher Ga contents a gradual narrowing of the band gap is observed, which is not related to changes in the amount of bonded hydrogen in the material.

(3) No changes in the hydrogen bonding nor in the effective void density are observed to be induced by the Ga in the material in the whole studied Ga concentration range.

(4) The position of the Fermi level, with respect to the conduction path levels, was determined from the conductivity results assuming conduction in extended states and a common constant prefactor for the activated conductivity for both electrons and holes. The total energy region swept by E_F in the studied Ga concentration range is about 0.3 eV, which takes into account the slight band-gap narrowing observed at the highest studied Ga concentrations.

(5) A semiquantitative electronic density of states distribution for the a-Ge:H and its evolution with Ga doping was deduced systematically by fitting an analytical model[34] to the optical absorption data (transmission and PDS). It was inferred that no Ga-induced changes in the DOS (and possibly no significant structural modifications) exist in the $0 \leq N_{Ga}/N_{Ge} < 4 \times 10^{-4}$ range. For higher Ga concentrations, a significant increase in the defect density and band-tail slope is observed with increasing N_{Ga}/N_{Ge}. This effect seems to be correlated with the Fermi level entering the lower part of the band gap and approaching the valence-band-tail region, the material becoming p type.

(6) The validity of the assumptions made for the analysis of the conductivity data was confirmed by evaluating the conductivity prefactor for both n- and p-type films, using the parameters for the density of states as derived from the absorption data. The results were found to be in the 140–260 $\Omega^{-1}\,cm^{-1}$range, which is in fair agreement with $\sigma_0 \approx 150\ \Omega^{-1}\,cm^{-1}$ proposed in the literature[31] and used in the present analysis. Similar σ_0 values were found for n-type and p-type samples, thus supporting previous assumptions of equal conductivity prefactor for electrons and holes[22] and in agreement with conclusions of both similar experimental work in a-Si:H (Ref. 28) and theoretical arguments.[31]

(7) Significant tendency for Ga segregation is observed for a-Ge:H having Ga atomic concentrations approaching 1×10^{-2}. This effect does not appear to contribute additional transport mechanisms to the conductivity.

ACKNOWLEDGMENTS

The authors are indebted to Professor J. Sanjurjo, UNICAMP, for the Raman scattering measurements, and to Professor F. Alvarez for discussions. This work has been partially founded by the Brazilian agencies FAPESP and CNPq.

[1] W.E. Spear and P.G. LeComber, Solid State Commun. **17**, 1193 (1975).
[2] A.J. Lewis, G.A.N. Connel, W. Paul, J.R. Pawlik, and R.J. Temkin, in *Tetrahedrally Bonded Amorphous Semiconductors*, edited by M.H. Brodsky, S. Kirkpatrick, and D. Wearie, AIP Conf. Proc. No. 20 (AIP, New York, 1974), p. 27.
[3] R.A. Street, Phys. Rev. Lett. **49**, 1187 (1982).
[4] N.F. Mott, Philos. Mag. **19**, 835 (1969).
[5] R.A. Street, *Hydrogenated Amorphous Silicon* (Cambridge University Press, New York, 1991).
[6] W. Paul, R.A. Street, and S. Wagner, J. Electron. Mater. **22**, 39 (1993).
[7] D.I. Jones, W.E. Spear, and P.G. LeComber, J. Non-Cryst. Solids **20**, 259 (1976).
[8] D. Hauschildt, M. Stutzmann, J. Stuke, and H. Dersch, Sol. Energy Mater. **8**, 319 (1982).
[9] M. Stutzmann, Philos. Mag. B **53**, L15 (1986).
[10] M. Stutzmann, D.K. Biegelsen, and R.A. Street, Phys. Rev. B **35**, 5666 (1987).
[11] F. Fajardo, D. Comedi, and I. Chambouleyron, Appl. Phys. Lett. **64**, 3275 (1994).
[12] F.H. Karg, B. Hirschauser, W. Kasper, and K. Pierz, Sol. Energy Mater. **22**, 169 (1991).
[13] T. Drüsedau and B. Schröder, J. Appl. Phys. **75**, 2864 (1994).
[14] W.A. Turner, S.J. Jones, D. Pang, B.F. Bateman, J.H. Chen, Y.M. Li, F.C. Marques, A.E. Wetsel, P. Wickboldt, W. Paul, J. Bodart, R.E. Norberg, I. ElZawawi, and M.L. Theye, J. Appl. Phys. **67**, 7430 (1990).
[15] F.C. Marques and I. Chambouleyron, *Proceedings of the 9th E.C. Photovoltaic Solar Energy Conference,* edited by W. Paltz, G.T. Wrison, and P. Helm (Kluwer, Dordrecht, 1989), p. 1042.
[16] D. Comedi, F. Fajardo, I. Chambouleyron, and M. Tabacniks, J. Vac. Sci. Technol. A **12**, 3149 (1994).
[17] R. Swanepoel, J. Phys. E **16**, 1514 (1983).
[18] C.J. Fang, K.J. Gruntz, L. Ley, M. Cardona, F.J. Demond, G. Muller, and S. Kabiltzer, J. Non-Cryst. Solids **35/36**, 255 (1980).
[19] K.L. Chopra, H.S. Randhawa, and L.K. Malhotra, Thin Solid Films **47**, 203 (1977).
[20] F. Fajardo, Ph.D. thesis, Universidade Estadual de Campinas, Unicamp, SP Brazil, 1994.
[21] V.P. Kesan, S.S. Iyer, and J.M. Cotte, Appl. Phys. Lett. **59**, 852 (1991).
[22] T. Drüsedau, A. Annen, H. Freisted, B. Schröder, and H. Oechsner, Philos. Mag. Lett. **66**, 175 (1992).
[23] S. Yamasaki, A. Matsuda, and K. Tanaka, Jpn. J. Appl. Phys. **21**, L789 (1982).
[24] W. Beyer, H. Wagner, and H. Mell, Solid State Commun. **39**, 375 (1981).
[25] T. Drüsedau, D. Pang, E. Sauvain, P. Wickboldt, E.Z. Liu, J.H. Chen, and W. Paul, in *Amorphous Silicon Technology—1993*, edited by E.A. Schiff, M.J. Thompson, A. Madan, K. Tanaka, and P.G. LeComber, MRS Symposia Proceedings No. 297 (Materials Research Society, Pittsburgh, 1993), p. 729.
[26] K. Eberhardt, M. Heintze, and G.H. Bauer, J. Non-Cryst. Solids **137/138**, 187 (1991).
[27] W. Beyer and H. Overhof, in *Hydrogenated Amorphous Silicon*, Part C: *Electronic and Transport Properties*, edited by J.I. Pankove, Semiconductors and Semimetals Vol. 21 (Academic Press, Orlando, 1984), Chap. 8.
[28] J. Kakalios and R.A. Street, Phys. Rev. B **34**, 6014 (1986).
[29] R.A. Street, J. Kakalios, C.C. Tsai, and T.M. Hayes, Phys. Rev. B **35**, 1316 (1987).
[30] R.A. Street and J. Zesch, Philos. Mag. B **50**, L19 (1984).
[31] H. Overhof and P. Thomas, *Electronic Transport in Hydrogenated Amorphous Semiconductors* (Springer-Verlag, Berlin, 1989).
[32] N. F. Mott, Philos. Mag. B **58**, 369 (1988).
[33] B. Ebersberger, W. Kruhler, W. Fuhs, and H. Mell, Appl. Phys. Lett. **65**, 1683 (1994).
[34] G.D. Cody, in *Hydrogenated Amorphous Silicon, Part B: Optical Properties*, edited by J.I. Pankove, Semiconductors and Semimetals Vol. 21 (Academic Press, New York, 1984).
[35] G.D. Cody, B.G. Brooks, and B. Abeles, Sol. Energy Mater. **8**, 231 (1982).
[36] J. Tauc, R. Grigorovici, and A. Vancu, Phys. Status Solidi **15**, 627 (1966).
[37] C.F.O. Graeff, M. Stutzmann, and K. Eberhardt, Philos. Mag. B **69**, 387 (1994).
[38] M. Stutzmann, J. Stuke, and H. Dersch, Phys. Status Solidi B **115**, 141 (1983).
[39] H. Curtins and M. Favre, in *Amorphous Silicon and Related Materials*, edited by H. Fritzche (World Scientific, Singapore, 1988), pp. 329–363.
[40] A.R. Zanatta and I. Chambouleyron, Phys. Rev. B **46**, 2119 (1992).
[41] B. Ebersberger, W. Kruhler, W. Fuhs, and H. Mell, *Proceedings of the 11th E.C. Photovoltaic Solar Energy Conference*, edited by L. Guimaraes *et al.* (Harwood Academic, Montreaux, Switzerland, 1992), P.S.598.
[42] K. Pierz, W. Fuhs, and H. Mell, Philos. Mag. B **63**, 123 (1991).
[43] K.J. Gruntz, L. Ley, M. Cardona, R. Johnson, G. Harbeke, and B. von Roedern, J. Non-Cryst. Solids **35&36**, 453 (1980).
[44] R.A. Street and K. Winer, Phys. Rev. B **40**, 6236 (1989).
[45] G.A.N. Connell and J.R. Pawlik, Phys. Rev. B **13**, 787 (1976).
[46] M. Stutzmann, Philos. Mag. B **60**, 531 (1989).